ISSUE: March 2024

Designing An Open-Source Power Inverter (Part 15): Transformer Magnetic Design For the Battery Converter

by Dennis Feucht, Innovatia Laboratories, Cayo, Belize

In this series on the design of an open-source power inverter dubbed the Volksinverter,[1-14] the two most recent parts explored the design of the power transfer circuit in the battery converter stage's power transfer circuit (Fig. 1). To implement this circuit, we considered the merits of three topologies, the boost push-pull (BPP), differential boost push-pull (DBPP) and bridge-switched common-passive circuits, ultimately sticking with the first option, the BPP (Fig. 2). As we look further into the design of this stage, we examine how to optimize the transformer design for this stage.

This and the next two parts of the Volksinverter design series present an example procedure—a design template—for optimizing the design of converter transformers for boost push-pull (BPP) power-transfer circuits. Optimizations include core selection, maximized primary-to-secondary power transfer, optimal winding area allocation, and minimized winding loss. The template is based heavily on previous derivations in other magnetics and Volksinverter series articles published in How2Power Today.

Transformer design follows the general procedure for magnetic component design given in Fig. 3. The Fig. 3 caption summarizes the major criteria of the optimizations. Magnetic design, which is the focus of this part, concerns determination of core material and size. The magnetic design is first because a core is first needed to determine the parameters of the windings.

Winding area allocation is considered under magnetic design because it affects *winding turns* N_p. (See the appendix.) N_p is an output parameter of magnetic (core) design and an important input to electrical (winding) design. Core choice is affected by winding currents and voltages from the circuit design.

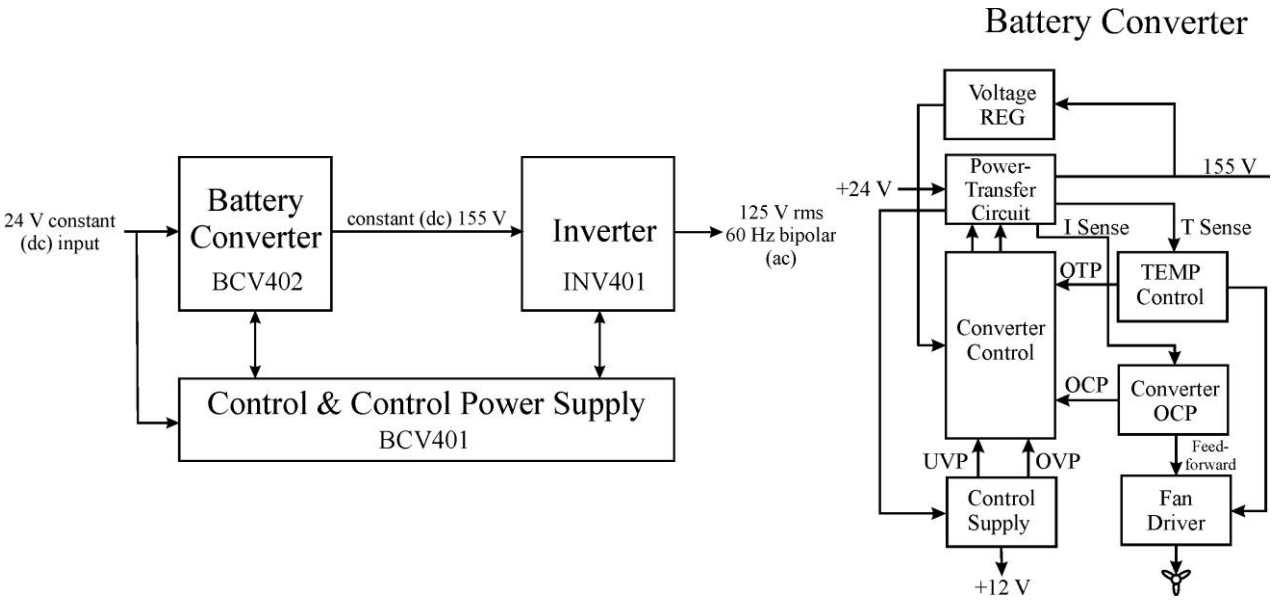

Fig. 1. The Volksinverter's system block diagram (left) and the BCV402 battery converter stage block diagram (right). Recent parts of this series weighed the merits of different topologies for the power transfer circuit in the battery converter stage. As we discovered, the boost push-pull (BPP), differential boost push-pull (DBPP) and bridge-switched common-passive circuits are all viable candidates, though we have settled on the boost push-pull as the primary choice for this design (see Fig. 2).

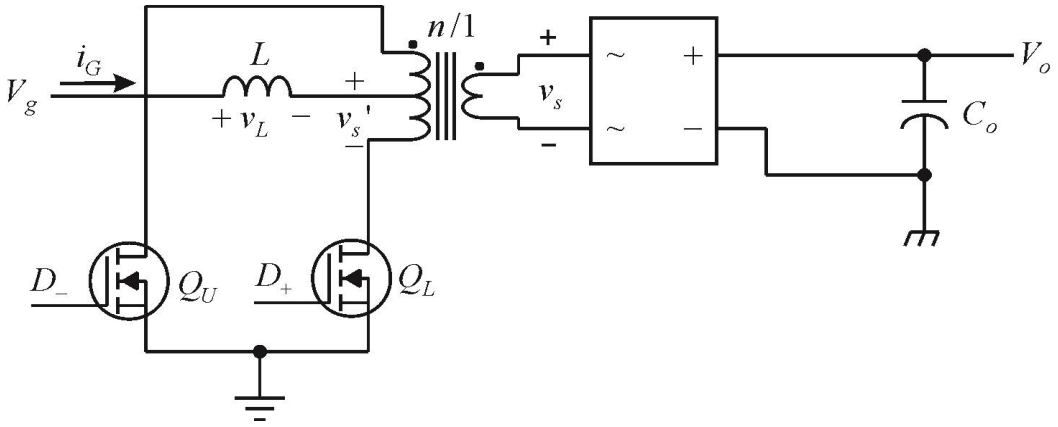

Fig. 2. The CA (boost) push-pull power-transfer circuit (BPP). The center-tapped primary winding is regarded as two identical but oppositely-phased primary windings. Each winding has a turns ratio of n = N_P/N_S. The MOSFET power switches are driven with duty-ratios D_+ and D_-. This part and the next two parts in this series present a design procedure for optimizing the transformer in this circuit.

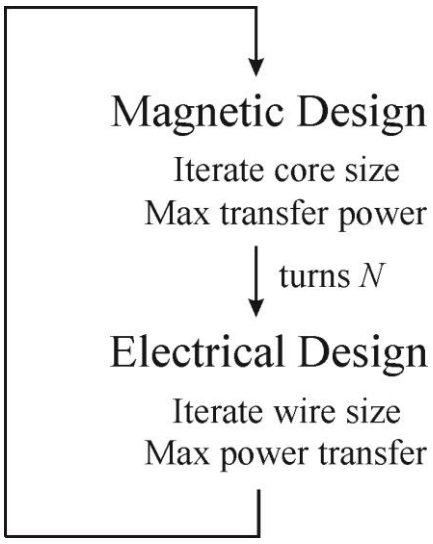

Fig. 3. General procedure for transductor (multi-winding magnetic component) design: magnetic design chooses core size to maximize transfer-power density; then winding design maximizes power transfer across windings. Magnetic design inputs choice of core material, shape, size, and temperature rise, and it outputs winding turns. Electrical (winding) design optimizes interwinding power transfer and minimizes winding loss. Bundle design includes strand and winding (sequential or multifilar) configuration, wire size, number of strands, and bundle twist pitch.

Circuit Constraints On Magnetic Design

What has been given in the specifications for the Volksinverter affect not only the circuit design but also the magnetics design: magnetic and electrical. The circuit-related parameters we need for magnetics design are those of the BPP power-transfer circuit: f_s = 150 kHz , T_s = 6.67 µs; n = 1/4 ; V_s = 160 V ; $V_g \in$ [20 V, 30 V] ; and $D' \in$ [0.5, 0.75]

Transformer design is constrained by the given circuit specifications. Circuit data for fs (full-scale) $\overline{P}_g$ = 333 W design are given in Table 1. The rated converter output voltage is V_o = 160 V. Then $V_s' = n \cdot V_s$ = 160 V/4 = 40 V. Given f_s input transfer power and voltage range, the average input current range

is given as I_g in Table 1. It also includes the design formulas from which the values of a given row are calculated.

Beneath Table 1 are equations from circuit design, derived in part 11 and listed here in one place for convenience. The need for circuit design formulas and their specified circuit constraints shows the importance of the interaction between circuit and magnetics designs. Circuit design is the initial step in magnetics design. Optimizing the circuit can require iteration of both circuit and magnetics designs as they relate to each other, each affecting the optimization of the other.

Table 1. BVC402 circuit design parameters and formulas.

V_g, V	20	25	30	Design Formula
I_g, A	16.67	13.32	11.1	$\bar{i}_g = I_g = \overline{P}_g / V_g$
D'	0.500	0.625	0.750	$D' = V_g / (n \cdot V_s)$
D	0.500	0.375	0.250	$D = 1 - D'$
$\bar{i}_Q$, A	12.5	10.0	8.33	$\bar{i}_Q = I_g / 2$
$\kappa_Q = \kappa_p$	1.225	1.275	1.323	$\kappa_p = \kappa_Q = \sqrt{1 + D'}$
$\tilde{i}_Q$, A	15.31	12.75	11.02	$\tilde{i}_p = \tilde{i}_Q = \kappa_Q \cdot (I_g / 2)$
$\bar{i}_s$, A	3.125	3.125	3.125	$\bar{i}_s = D' \cdot n \cdot I_g$
κ_s	1.414	1.265	1.155	xfmr $\kappa_s = 1 / \sqrt{D'}$
$\tilde{i}_s$, A	4.42	3.95	3.61	$\tilde{i}_s = \kappa_s \cdot \bar{i}_s = n \cdot I_g \cdot \sqrt{D'}$
$\bar{i}_D$, A	1.56	1.56	1.56	FWB $\bar{i}_D = \bar{i}_s / 2$
FWB κ_D	2.00	1.79	1.63	FWB $\kappa_D = \sqrt{2 / D'}$
FWB $\tilde{i}_D$, A	3.12	2.79	2.54	FWB $\tilde{i}_D = \kappa_D \cdot \bar{i}_D$
FWB κ_{QD}	2.45	2.28	2.16	FWB $\kappa_{QD} = \kappa_Q \cdot \kappa_D$
$V_s' - V_g$, V	20	15	10	$n \cdot V_s - V_g$
t_{on}, µs	3.33	2.50	1.67	$t_{on} = D \cdot T_s$
$\Delta\lambda_L$, V·µs	66.7	62.5	50.0	$\Delta\lambda_L = V_g \cdot (D \cdot T_s)$
$\overline{P}_L$, W	166.5	125	83.25	$(V_s' - V_g) \cdot D' \cdot I_g = D \cdot \overline{P}_g$

$$D' = 1 - D = \frac{V_g}{V_s'} \; ; \; V_s' = n \cdot V_s \; ; \; n = \frac{N_p}{N_s}$$

$$\tilde{i}_Q = \tilde{i}_p = \frac{I_g}{2} \cdot \sqrt{1 + D'} \; ; \; \bar{i}_Q = \bar{i}_p = \frac{I_g}{2} = D \cdot \frac{I_g}{2} + \tfrac{1}{2} \cdot D' \cdot I_g \; ; \; \kappa_p = \sqrt{1 + D'} \; ; \; \kappa = \frac{\tilde{i}}{\bar{i}} = \frac{\text{rms}}{\text{avg}} \quad I_{g\max} = \frac{2 \cdot \tilde{i}_{p\max}}{\sqrt{1 + D'_{\min}}}$$

$$\tilde{i}_s = n \cdot I_g \cdot \sqrt{D'} \; ; \; \bar{i}_s = n \cdot I_g \cdot D' \; ; \; \kappa_s = 1/\sqrt{D'} \; ; \; \bar{i}_D = n \cdot I_g \cdot \sqrt{D'/2} \; ; \; \kappa_D = \sqrt{2/D'}$$

$$\tilde{v}_p = \sqrt{\frac{D'}{2}} \cdot V_s' = \sqrt{\frac{D'}{2}} \cdot \frac{V_g}{D} = \frac{V_g}{\sqrt{2 \cdot D'}} \; ; \; \bar{v}_p = \tfrac{1}{2} \cdot D' \cdot V_s'$$

The BPP magnetic frequency is $f = f_s/2$ = 75 kHz. Ferrite is chosen because its ripple factor $\gamma = \hat{i}_{m\sim} / \bar{i}_m = \tfrac{1}{2} \cdot \Delta i_m / \bar{i}_m$ best matches transformer bipolar waveforms over a (unipolar) half-cycle. Transformer waveforms are symmetric and bipolar; $\gamma \to \infty$ because the cycle average is zero, but each square-wave half-cycle has $\gamma = 1$. (For a sine-wave, $\gamma = \tfrac{1}{2}/(2/\pi) = \pi/4 \approx 0.7854 >> 0$.)

Of commercial cores, ferrites have the highest γ_{opt}; MnZn ferrite $\gamma_{opt} \approx 0.4$. The choice of core material for PWM-switch converter transformers is therefore a clear one.

Transformer Core Size

Transformers primarily transfer energy instead of storing it. Core size is based on average primary-winding design power $\bar{P}_{pd}$ and a core size that can sustain it becomes a possible choice. The specification of primary design power as $\bar{P}_{gd} = \bar{P}_{pd}$ = 500 W leads to a choice of core size iterated in design.

The Innovatia magnetics design procedure *begins* with a guess at core size because size is constrained by both core and winding design and cannot be known at the outset of the procedure. Some core catalogs give graphs scaling transfer power against various cores. Experience provides the best guess. Wrong guesses induce iteration.

Because both window area A_w and the magnetic-path cross-sectional area A of a core can be related to core size, the area-product method[15] is sometimes applied because the initial choice of a size need not be too accurate. (The area-product method is fraught with assumptions;[15] do not depend on it for accuracy.) The area-product method estimates a core size from area product $A \cdot A_w$ of magnetic core cross-sectional area A and (bobbin) window area A_w and gives an expression for the fs input power $\bar{P}_g$. It must then be re-scaled over the V_g range for design power by the factor $\bar{P}_{gd} / \bar{P}_g$;

$$\bar{P}_g = (A \cdot A_w) \cdot \left(\frac{k_p \cdot \tilde{j}_c \cdot (2 \cdot \hat{B}_\sim) \cdot f}{\kappa_p \cdot D} \right)$$

The area product is proportional to $\bar{P}_g$ if the parameters in the enclosed expression are constant. However, $k_p \approx 0.66$ for 24 AWG varies with wire size; $\tilde{j}_c \approx 4.5$ A/mm^2 (1 cm^4, Cu) varies with core size; $\kappa_p \approx 1.25$ varies with current ripple waveshape; and D ($\approx D_{opt} = 0.382$) varies with converter operating-point and V_g. $\hat{B}_\sim \cdot f$ varies with core material and is a circuit-related dynamic performance parameter.

The optimal operating-point frequency for a core is where maximum power transfer can occur and that is at maximum $\hat{B}_{\sim} \cdot f$. Ferroxcube 3C90 ferrite material (or equivalent) has peak $\hat{B}_{\sim} \cdot f$ around 20 mT·MHz and is a function of *f* which for the Volksinverter is 75 kHz. Then $\hat{B}_{\sim}$ = 267 mT.

However, there is another way to size ferrite cores. Ferrite material B_{sat} or $\overline{H}_{sat}$ is nearly constant, allowing $\hat{B}_{\sim}$ = Δ*B*/2 to be varied by the air gap. At a given *f* and $\overline{P}_g$, transfer-power density varies with $\hat{B}_{\sim}$ which varies inversely with permeability μ or field inductance $\mathcal{L}$. As $\overline{P}_g$ increases, $\mathcal{L}$ must be decreased. A formula derived from the basic transfer-power field equation, Magnetic Ohm's Law $\phi = \mathcal{L} \cdot Ni$, for maximum $\mathcal{L}$ [16] is

$$\mathcal{L} \le [2 \cdot (\hat{B}_{\sim} \cdot f) \cdot A] \cdot [\overline{B} \cdot A] / \overline{P}_{pd}$$

$\hat{B}_{\sim}$ for a transformer is that of magnetizing inductance; the transfer fields of primary and secondary windings cancel, leaving the magnetizing field. Cores in a core catalog with $\mathcal{L}$ values low enough to support $\overline{P}_{pd}$ are design options. The choice of $\mathcal{L}$ also affects turns N_p and is constrained by the maximum turns N_w that the window can accommodate. Core sizing therefore is an inherently iterative aspect of design and after having iterated through previous designs, an intuition develops for what size is about right for a given transfer power.

For transfer power over 500 W, it is distributed among multiple transformers for optimal thermal design. The area-product formula offers a guide. The first choice of a core size is the ETD34-3C90 for Volksinverter $\overline{P}_g$ = 333 W design—a transfer power somewhat higher than the area-product formula gives. Transformer and inductor *design-power* values[17-19] over V_g (from part 12) are

$$\overline{P}_{Ld} = \frac{1}{4} \cdot \frac{V_s'}{V_{g\min}} \cdot \overline{P}_g = (0.5) \cdot (333\ \text{W}) = \mathbf{167\ W}$$

$$\overline{P}_{pd} = \sqrt{\frac{1}{2} \cdot \left(\frac{V_{g\max}}{V_{g\min}} \right) \cdot \left(1 + \frac{V_s'}{V_{g\min}} \right)} \cdot \overline{P}_g = (1.5) \cdot (333\ \text{W}) = \mathbf{500\ W}$$

If the calculated static power constrained by winding thermal limits for current in the core window is less than needed to achieve $\overline{P}_{gd} = \overline{P}_{pd}$, then iteration to a larger core size is the next step. However, it might be worthwhile to follow the procedure somewhat further to the winding design to determine whether the $\mathcal{L}$ range for available air gaps will allow the chosen core to transfer the $\overline{P}_{pd}$ value. Then a decision is made based on how well the winding design alternatives of available $\mathcal{L}$ for the given core size compare for $\overline{P}_{pd}$.

The Volksinverter project choice of core shapes are ETD and EER. They are higher in core loss than comparable PQ or RM shapes. However, they increase core options for the prototype design. A photograph of the four chosen cores with bobbins having the same circuit-board footprint is shown in Fig. 4 mounted on bare BCV402 circuit-boards.

Three of these have vertical bobbins that minimize board area for a given core volume. But they constrain winding design in that if both ends of a winding are to have minimal lead length, the winding must have an even number of layers to bring both ends to the bottom of the winding window.

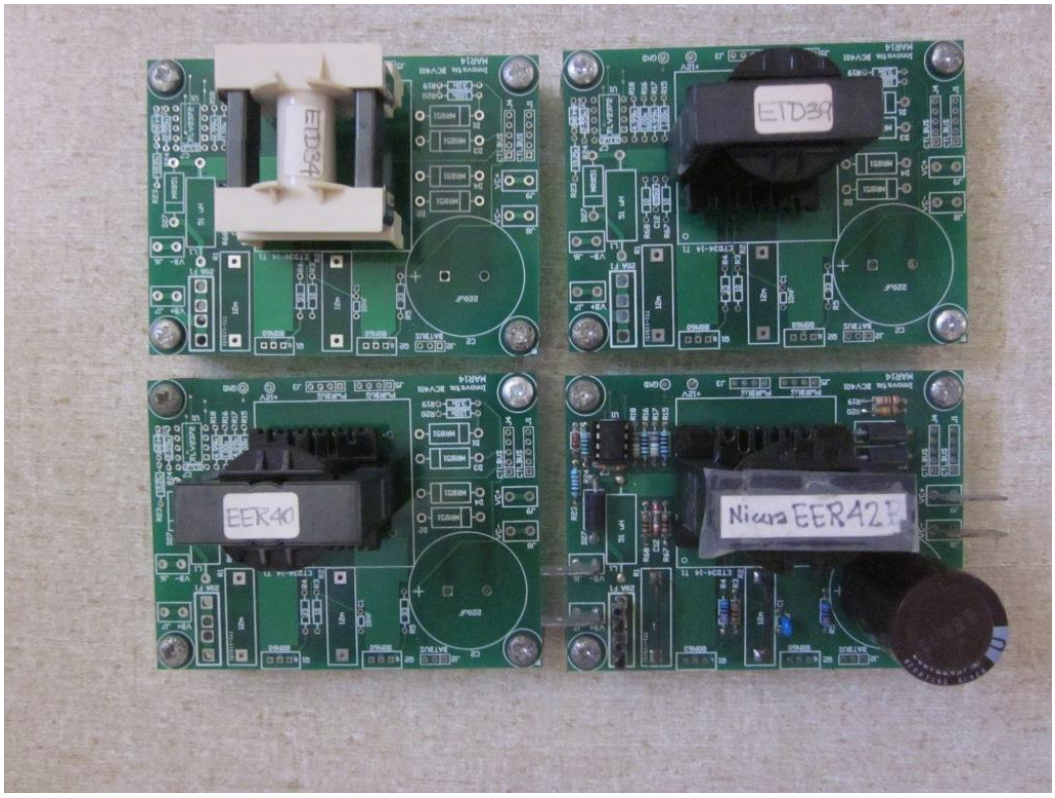

Fig. 4. Four board-interchangeable core alternatives have the same bobbin footprint. Three vertical-mount cores (black) are largest and occupy the same board area by being higher. The storage capacitor (lower-right) is highest.

Table 2 lists the four core choices (from Innovatia inventory) for the four transformer designs of Fig. 4. By choosing commercial parts, magnetic design reduces to selection of core material, shape, size, field inductance $\mathcal{L}$ (or permeability μ) and turns N_p. The Table 2 power values are initial design estimates based on $V^{2/3}$ scaling of ETD34.

Table 2. BCV402 core alternatives with initial power-transfer estimates.

Core Type	Volume V, cm^3	Max. power transfer $\overline{P}_g$, W	Design power $\overline{P}_{pd}$, W	Power-transfer density $\overline{P}_g / V$, W/cm^3
EER42	19.16	452	678	23.6
EER40	14.587	413	620	28.3
ETD39	11.5	382	573	33.2
ETD34	7.64	333	500	43.6

The transformer design template is that of an ETD34-3C90 core though the same procedure applies to the others:

ETD34 parameters: V = 7.64 cm^3; A = 97.1 mm^2; Ferroxcube bobbin A_w = 123 mm^2, w_w = 20.9 mm, and h_w = 6.0 mm.

Window dimensions are those of the bobbin (coil-former); its window dimensions are used for winding design.

Core shape does not change the design procedure. If you have a large inventory of suboptimal cores that you want to reduce (as does Innovatia) by using them in prototyping or for low-volume or custom products, they will result in higher core loss. This can affect core size and will affect the optimization of winding power transfer and thus the choice of winding resistance, but otherwise the design procedure remains the same as for the ETD34 core.

Unavoidable magnetizing current i_m and A_w of the electrical design limit minimum core size. MnZn ferrite cores typically have $\Delta B_{sat} \approx 0.35$ T that limits $\hat{i}_m$. Core loss limits i_m by ripple amplitude $\hat{i}_{m\sim}$. The i_m ripple factor over a half-cycle is

$$\gamma_m = \hat{i}_{m\sim} / \bar{i}_m = \text{ferrite } \gamma_{opt}$$

γ_m has (as we will see later, under "Turns") optimally near-equal transformer minimum-turns limits N_λ of core loss and N_i of core saturation. Core size is reduced whenever they are maximized to achieve maximum magnetizing power density in the core and maximize core utilization.

Magnetic Thermal Design

The next step in magnetic design is to find the allowable core power-loss density $\bar{p}_c$ from thermal resistance and allowable ΔT above maximum ambient temperature. A core *shape-based thermal model*[20] starts with the analytically simplest and worst-case thermal shape: the sphere. Actual cores have an improvement over that of a sphere of *thermal shape factor* Ξ_θ. That is, allowable core-loss density can be increased for a given maximum ΔT of temperature over that of a spherical core by Ξ_θ so that the maximum allowable

$$\bar{p}_c \le \Xi_\theta \cdot (1 - \tfrac{1}{2} \cdot f_w) \cdot \bar{p}_c(\text{sphere})$$

The *winding configuration factor* f_w is the fraction of heat from the windings that goes through the core. Ξ_θ and f_w are both based on transductor geometry and are independent of core size. Given f and this core-loss value, $\hat{B}_\sim$ can be read from the core-loss catalog horizontal axis of the $\bar{p}_c(\hat{B}_\sim, f)$ material graph. Then core power loss $\bar{P}_c = \bar{p}_c \cdot V$ for core size of volume V.

Core temperature rise ΔT, specified to find $\bar{P}_c$, limits core size as determined by f_s, ΔB_m, and core thermal resistance. Field inductance $\mathcal{L}$ (= A_L in core catalogs) determines the maximum allowable $\hat{B}_{m\sim} = \Delta B_m/2$ caused by Δi_m. $\mathcal{L}$ is maximized to minimize Δi_m ripple while keeping transfer power ≥ $\bar{P}_{pd}$.

Two thermal models exist in the literature. The one for windings is the

$$\text{wire current-density thermal size factor} = \tilde{J} / \tilde{J}_0 = (A \cdot A_w / \text{cm}^4)^{-1/8} = 0.978\ ;\ \tilde{J}_0 = 4.5\ \text{A/mm}^2,\ 25\ ^\circ\text{C, Cu}$$

The other is for the core. Thermal models are either network or shape-based. The shape-based model has fewer assumptions (or approximations) and has two design formulas. Given natural (still air) convection,

$$r = \left(\frac{3 \cdot V}{4 \cdot \pi}\right)^{1/3} \approx 0.6204 \cdot V^{1/3};\ \bar{p}_c(\text{sphere}) = \frac{\Delta T}{(8.33\,\text{cm} \cdot \text{K/W}) \cdot r^2 + (167\,\text{cm}^2 \cdot \text{K/W}) \cdot r} = \frac{40\,\text{K}}{240.7\ \text{W/cm}^3}$$

ΔT = 40 K is chosen based on the catalog plot of $\bar{p}_c(T)$. The temperature of its minimum is where loss begins to increase with temperature—a positive TC that can cause thermal runaway. Hence, the temperature of minimum loss is considered the maximum allowable temperature, and for ferrite it is typically about 90°C. Then if the maximum operating temperature is specified as 50°C, the difference is ΔT = 40°C = 40 K. Then substituting,

$$\bar{p}_c(\text{sphere}) = 166\ \text{mW/cm}^3;\ f_w = \text{fraction of winding heat through core} \approx \tfrac{1}{3};\ \Xi_\theta(\text{ETD}) = 1.8$$

Core winding geometry affects heat paths and is included as parameter f_w, an approximated fraction of winding heat that passes through the core. For pot cores, all the winding heat goes through the core and f_w = 1. The opposite extreme is toroids where all the core heat goes through the windings, and f_w = 0. For ETD and EER cores, $f_w \approx \tfrac{1}{3}$. For equal core and winding loss, the core-winding configuration factor ≈ (1 – ½·f_w).[21] Allowable core power-loss density is

$$\bar{p}_c = [(1-\tfrac{1}{2}\cdot f_w)\cdot\Xi_\theta]\cdot\bar{p}_c(\text{sphere}) = [(5/6)\cdot(1.8)]\cdot(166\ \text{mW/cm}^3) = (1.5)\cdot(166\ \text{mW/cm}^3) = 249\ \text{mW/cm}^3$$

from which it follows that core loss for the selected ETD34 core is

$$\bar{P}_c = \bar{p}_c \cdot V = (249\,\text{mW/cm}^3)\cdot(7.64\,\text{cm}^3) = 1.90\ \text{W}$$

Forced-air convection from fans decreases heat-sink-to-ambient thermal resistance and increases allowable $\bar{p}_c$ by decreasing the convection coefficient of 167 cm²·K/W. Heat-sink catalogs have graphs of heat-sink-to-air thermal resistance $R_{\theta SA}$ as a function of air speed that show the reduction of $R_{\theta SA}$ from still air. Fans have air-speed ratings. The effective $R_{\theta SA}$ is estimated based on air flow where the transformers are placed on the circuit-board relative to fan position. Forced-air thermal modeling is thereby complicated; the still-air $\bar{p}_c$ is a conservative minimum.

From the magnetic design, our first derived parameter is winding resistance. Average natural-convection (still-air) core power-loss and hence allowable maximum winding resistance referred to the primary winding is

$$\text{Per-winding optimal } R_{wp} = \frac{1}{2}\cdot\frac{(\bar{P}_c\cdot\psi_{\max})/2}{\tilde{i}_p^{\,2}} \approx \frac{1}{2}\cdot\frac{(\bar{P}_c/2)}{\tilde{i}_p^{\,2}} = \frac{0.476\,\text{W}}{\tilde{i}_p^{\,2}},\ \bar{P}_w \approx \bar{P}_c \text{ at } \psi_{\max} \approx \eta_{\max} \approx 1, \beta_p \approx 0$$

The power-loss optimizations are based on core and winding losses as about equal ($\bar{P}_w \approx \bar{P}_c$), that primary and secondary winding losses be split equally between them, $\bar{P}_{wp} = \bar{P}_{ws} = \bar{P}_c/2$, and that losses of the primary windings also be split equally (½). Equivalent primary-referred core resistance R_c in the transformer circuit model is needed for transfer efficiency calculations in winding design (over the V_g or D range), based on core loss. R_c varies over V_g as

$$R_c = \frac{V_g^2}{\bar{P}_c} = [211\Omega, 474\Omega],\ V_g \in [20\ \text{V}, 30\ \text{V}]$$

Turns

Besides the core, the only limitation on power transfer across transformer windings is power loss in the windings. They are limited by window area A_w. Core size is also limited by magnetizing flux, which is more basically limited by core power-loss density $\bar{p}_c$.

The transfer flux of primary and secondary windings cancels, leaving a net flux in the core caused by magnetizing current. During on-time, the primary windings are shorted with no voltage across primary-referred

magnetizing inductance L_{mp}. During off-time, magnetizing flux transitions by ΔB_m between $+\hat{B}_{m\sim}$ and $-\hat{B}_{m\sim}$. The magnetizing current waveform $i_m(t)$ is a trapezoidal-wave and not a square-wave or sine-wave. Core loss data is given for sine-waves, and without constructing a Fourier series for $B_m(t)$, our best estimate of core-loss density is based on sine-wave data, graphed in core catalog materials sections as $\overline{p}_c(\hat{B}_{\sim}, f)$.

Increased frequency places greater performance demand on the switches and their drivers, and in keeping with the Volksinverter design goal of commodity (low-cost, widely available) parts, the older gate drivers with modest drive current i_G (< 2 A) are retained in the design. (High di_G/dt not only requires low parasitic gate-source input-loop inductance, it also results in appreciable average gate-drive current that can rival the base current of Darlington Si or SiC BJTs!) Commercialization of the Volksinverter might benefit from refinement of gate-drive design choices.

Given f and $\overline{p}_c$ from the core thermal calculations, $\hat{B}_{\sim}$ is found on the graphs. On the 3C90 plot for 75 kHz and 249 mW/cm^3, (rounding down 10% for non-sine) $\hat{B}_{\sim} \approx 0.18$ T. Then the power-loss lower bound on N_p is

$$N_\lambda = \frac{\Delta\lambda}{\Delta\phi(\overline{p}_c)} = \frac{V_s' \cdot [D_{\max}' \cdot T_s]}{[2 \cdot \hat{B}_{\sim}(249\,\mathrm{mW/cm^3})] \cdot A} = \frac{(40\,\mathrm{V}) \cdot [(0.75) \cdot (6.67\,\mu\mathrm{s})]}{2 \cdot (0.18\,\mathrm{T}) \cdot (97.1\,\mathrm{mm^2})} = \frac{200\,\mu\mathrm{V \cdot s}}{35\,\mu\mathrm{V \cdot s}} = 5.71 \rightarrow 6$$

Core saturation is the other limiting core parameter that limits the maximum N for a given ΔB_i to

$$N_i = \frac{\Delta\lambda}{\Delta\phi_i} = \frac{200\,\mu\mathrm{V \cdot s}}{(0.35\,\mathrm{T}) \cdot (97.1\,\mathrm{mm^2})} = \frac{200\,\mu\mathrm{V \cdot s}}{34.0\,\mu\mathrm{V \cdot s}} = 5.88 \rightarrow 6$$

The onset of saturation is difficult to determine, even for ferrites. The $B(H)$ catalog curves are not very indicative of it. The graph to use is $\mu_r(\hat{B}_{\sim})$. On these plots, μ peaks around the value to use for saturation, where $\hat{B}_{\sim} \approx 175$ mT for 3C90. Then $\Delta B_{\sim} = 0.35$ T. Driving the core above this value enters a region where μ_r (and $\mathcal{L}$) decrease with increasing current. In it, superlinear $i(t)$ can cause control problems.

The small-ripple approximation does not apply to transformers because symmetric bipolar waveforms are all ripple with zero average winding current and voltage. Primary-winding magnetizing-current ripple $\Delta i_{mp} = \Delta\lambda_p/L_p$ affects field-current ripple ΔNi (which is otherwise determined by inductor current), and N_i changes from a maximum bound on N to another minimum;[22]

$$N \le \frac{\Delta N i_m}{\Delta i_m} = \frac{\Delta\phi_{im} / \mathcal{L}}{\left(\frac{\Delta\lambda_m}{N^2 \cdot \mathcal{L}}\right)},\ \mathcal{L} = \text{field inductance } (\mathrm{A_L})$$

Solving for N,

$$N \ge N_i = \frac{\Delta\lambda_m}{\Delta\phi_{im}} = \frac{\hat{\lambda}_m}{\hat{\phi}_{im}}\ ,\ \hat{\phi}_{im} = \hat{B}_m \cdot A$$

Hence N_i becomes another minimum, and for a transformer,

$$\boxed{N_p = \max\{N_\lambda, N_i\} = 6}$$

Furthermore, the major loop of the core $B(H)$ curve is traversed between $\pm B_{sat}$ which at maximum flux drive is also the B ripple $\hat{B}_{m\sim}$. MnZn ferrites characteristically have $B_{sat} \approx 175$ mT. The symmetric bipolar current and

voltage waveforms of transformers have half-cycle $\gamma \rightarrow 1$ which drives the minimum turns N_λ and N_i to the same (optimized) value, and magnetizing power density in the core is maximized. This sets the core power-loss limit. (Transformer winding loss is usually the overall limiting parameter.)

In the case of the ETD34 core, $\hat{B}_{m\sim} \approx B_{sat} \approx 175$ mT and ETD34-3C90 $\overline{p}_c \approx 249$ mW/cm^3. Because $N_\lambda \approx N_i$, i_{mp} achieves maximum power density in the core, indicating full core utilization for $N_p = 6$. In other words, driving the core harder will drive it out of the acceptable operating region of both core loss and saturation. Finally, the secondary turns number is

$$\boxed{N_s = (1/n)\cdot N_p = 4\cdot 6 = 24}$$

Winding turns for primary and secondary windings have now been determined.

If f_s is increased, thereby increasing f, then $\Delta\lambda$ is decreased, and N_p and N_s decrease, leaving more window area for larger wire and more power transfer. The circuit tradeoff is that switching time becomes a greater fraction of T_s as does switching loss. Gate-drive current must also increase to compensate, and parasitic circuit inductance becomes limiting.

We now have all the derived parameters required to proceed to transformer electrical (winding) design. It involves a choice of geometric configuration of the windings, calculation of optimal area allotments for each winding, and then the design of each winding as a configured number of strands of wire of a given size.

Electrical design is more involved than magnetic design because the possible alternative plans for windings are greater. Apart from venturing into core design itself and apart from custom core optimization—either by stacking toroids, introducing a gap between core legs or mixing E and I sections—core selection is confined to what is commercially available from core manufacturers.

References

1. "Designing An Open-Source Power Inverter (Part 1): Goals And Specifications" by Dennis Feucht, How2Power Today, May 2021.
2. "Designing An Open-Source Power Inverter (Part 2): Waveshape Selection" by Dennis Feucht, How2Power Today, September 2021.
3. "Designing An Open-Source Power Inverter (Part 3): Power-Transfer Circuit Options" by Dennis Feucht, How2Power Today, April 2022.
4. "Designing An Open-Source Power Inverter (Part 4): The Optimal Power-Line Waveshape" by Dennis Feucht, How2Power Today, May 2022.
5. "Designing An Open-Source Power Inverter (Part 5): Kilowatt Inverter Circuit Design" by Dennis Feucht, How2Power Today, July 2022.
6. "Designing An Open-Source Power Inverter (Part 6): Kilowatt Inverter Control Circuits" by Dennis Feucht, How2Power Today, August 2022.
7. "Designing An Open-Source Power Inverter (Part 7): Kilowatt Inverter Magnetics" by Dennis Feucht, How2Power Today, September 2022.
8. "Designing An Open-Source Power Inverter (Part 8): Converter Control Power Supply" by Dennis Feucht, How2Power Today, November 2022.
9. "Designing An Open-Source Power Inverter (Part 9): Magnetics For The Converter Control Power Supply" by Dennis Feucht, How2Power Today, December 2022.
10. "Designing An Open-Source Power Inverter (Part 10): Converter Protection Circuits" by Dennis Feucht, How2Power Today, February 2023.

11. "Designing An Open-Source Power Inverter (Part 11): Minimizing Switch Loss In Low-Input-Resistance Converters" by Dennis Feucht, How2Power Today, March 2023.
12. "Designing An Open-Source Power Inverter (Part 12): Sizing The Converter Magnetics" by Dennis Feucht, How2Power Today, March 2023.
13. "Designing An Open-Source Power Inverter (Part 13): The Differential Boost Push-Pull Power-Transfer Circuit" by Dennis Feucht, How2Power Today, June 2023.
14. "Evaluating Waveform Form Factors Of FW And HW Rectifiers In SMPSs" by Dennis Feucht, How2Power Today, April 2023.
15. "Area-Product Method Can Simplify Core Selection—But Beware Of The "Constants" by Dennis Feucht, How2Power Today, August 2015.
16. "Core Sizing", *Power Magnetics Design Optimization*, Innovatia, pages 374-377.
17. "Sizing Your Power Converter's Magnetics (Part 1): Inductor Power Rating With Fixed Input Voltage" by Dennis Feucht, How2Power Today, April 2016.
18. "Sizing Your Power Converter's Magnetics (Part 2): Inductor Power Rating With An Input Voltage Range" by Dennis Feucht, How2Power Today, May 2016.
19. "Sizing Your Power Converter's Magnetics (Part 3): Transformer Power Rating With An Input Voltage Range" by Dennis Feucht, How2Power Today, June 2016.
20. "How To Choose Magnetic Core Size" by Dennis Feucht, How2Power Today, May 2013. This article explains the shape-based thermal model.
21. "Transformer Design (Part 1): Maximizing Core Utilization" by Dennis Feucht, How2Power Today, January 2018.
22. Power Magnetics Design Optimization, Innovatia, pages 89, 90.

Appendix—The Multiple Meanings Of Turns

The practice in science and engineering is to refer to physical entities such as flowing charge or closed loops of wire with the same words as apply to their quantification. Because they are so closely related this does not cause confusion. The definition of a quantity includes what is being quantified. For instance, current is by definition the rate of charge flowing in a conductor, with units of amperes. But to refer to the moving charge itself as current causes no confusion because the moving charge and its value (current) are so closely related. Thus, current refers to both the moving charge and its value in amperes.

Similarly, closed loops of wire or turns are not confused by their quantification as the number of them. Hence, to say "turns N" where N is the unitless value of the turns should not cause confusion either. In this case, the turns themselves and the number N of them are both a part of the definition of turns, and we can refer to either the physical loops themselves or the number of them as turns.

About The Author

Dennis Feucht has been involved in power electronics for 40 years, designing motor-drives and power converters. He has an instrument background from Tektronix, where he designed test and measurement equipment and did research in Tek Labs. He has lately been working on projects in theoretical magnetics and power converter research.

For further reading on magnetics design, see the How2Power Design Guide, locate the Design Area category and select "Magnetics".